ACS OMEGA

Article

http://pubs.acs.org/journal/acsodf

$Bi_2O_2CO_3$ Nanosheets as Electrocatalysts for Selective Reduction of CO_2 to Formate at Low Overpotential

Weixin Lv,[†] Jingjing Bei,[†] Rui Zhang,*[,†] Wenjuan Wang,[†] Fenying Kong,[†] Lei Wang,[‡] and Wei Wang*[,†]

[†]School of Chemistry and Chemical Engineering, Yancheng Institute of Technology, 9 Yingbin Road, Yancheng 224051, P. R. China

[‡]Key Laboratory of Functional Inorganic Material Chemistry, Ministry of Education of the People's Republic of China, Heilongjiang University, 74 Xuefu Road, Harbin 150080, P. R. China

ABSTRACT: Electrochemical reduction of carbon dioxide (CO_2) to formate is energetically inefficient because a high overpotential (>1.0 V) is required for most traditional catalysts. In this work, $Bi_2O_2CO_3$ (BOC) nanosheets were synthesized as electrocatalysts of CO_2 reduction for the first time. Additionally, BOC decorated on the glassy carbon electrode was reduced in situ to metal Bi (RB) for comparing the catalytic performance toward CO_2 reduction to that of BOC. The maximum faradaic efficiency of BOC was 83% at an overpotential of 0.59 V, which is a little lower than that of RB (90% obtained at the overpotential of 0.99 V). However, the overpotential for the reduction of CO_2 to formate on BOC is obviously decreased compared to that on RB. After 27 h of electrolysis, approximately 80% formate selectivity was obtained using the BOC catalyst. According to the experimental results and the related literature, a new mechanism for the CO_2 reduction reaction on BOC was proposed, which may play a guiding role in future catalyst design.

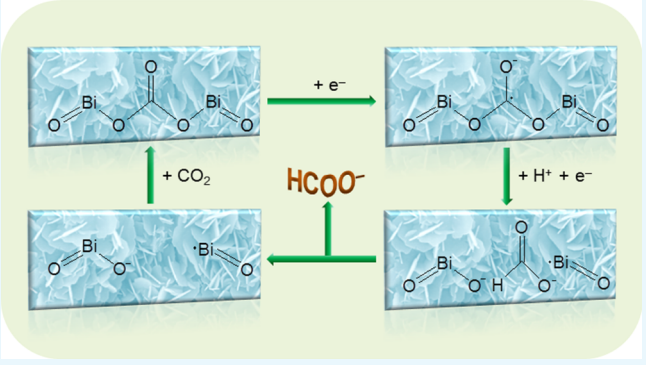

1. INTRODUCTION

The abundant use of fossil fuels has accelerated the depletion of these nonrenewable resources and has led to excessive emission of carbon dioxide (CO_2).[1] Converting CO_2 into fuels and useful industrial chemicals using solar and/or wind energy sources is an ideal solution for reducing CO_2 emissions.[2−6] Figure 1 shows the evolution of publications on electrochemical reduction of CO_2 since the year 1980 (sources: Web of science, Thomson Reuters). Over the past few years, especially starting from the year of 2009, research on the electrochemical reduction of CO_2 has received much attention.

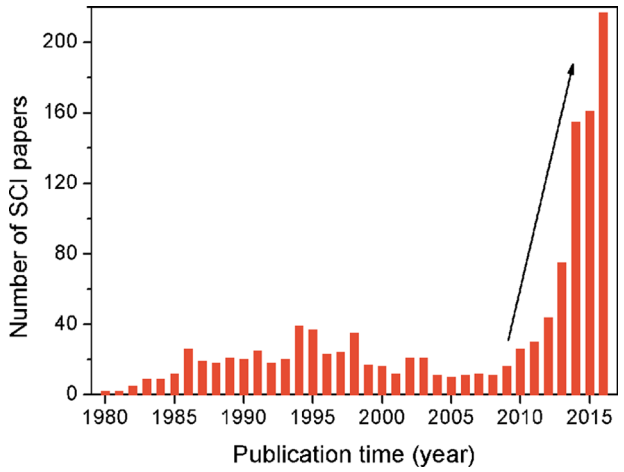

Figure 1. Number of publications dedicated to research on electrochemical reduction of CO_2 since the year 1980.

In aqueous solution, the hydrogen evolution reaction (HER) competes with the CO_2 reduction reaction on the cathode.[7,8] Researchers have found that Sn, In, and Pb electrodes, which possess high hydrogen overpotentials, are passivated for the HER but are active for the CO_2 reduction reaction. Additionally, a faradaic efficiency (FE) higher than 80% can be easily obtained under optimum electrolysis conditions for these metal electrodes.[9,10] The CO_2 reduction process has largely been stymied by an impractically high overpotential (>1.0 V), which is necessary to drive the process on traditional catalysts (including metal plates, nanosized metal particles, and carbon-supported metal catalysts).[11−17] Developing highly active catalysts for the reduction of CO_2 to formate at a low overpotential is thus the main challenge.

The overpotential for the conversion of CO_2 into fuels should decrease upon stabilizing the intermediate. Rosen et al. reported that 1-ethyl-3-methylimidazolium tetrafluoroborate in the electrolyte can form a complex with $CO_2^{\bullet-}$, which can decrease the overpotential for the reduction of CO_2 to CO by lowering the free energy of formation of the $CO_2^{\bullet-}$ intermediate.[18] For the CO_2 reduction reaction, it is commonly

Received: April 11, 2017
Accepted: May 26, 2017
Published: June 8, 2017

DOI: 10.1021/acsomega.7b00437
ACS Omega 2017, 2, 2561−2567

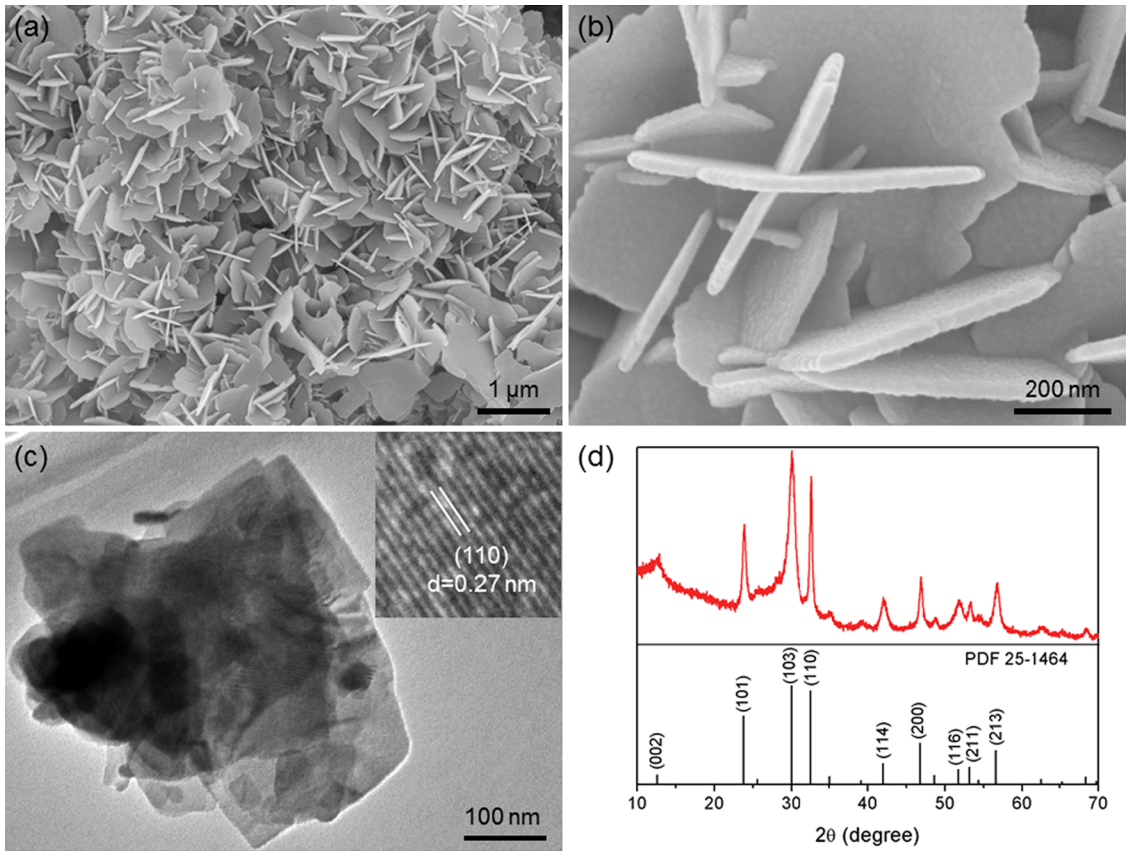

Figure 2. (a, b) Scanning electron microscopy (SEM) images of BOC. (c) TEM image of BOC; the insert of (c) is the corresponding HRTEM image. (d) XRD pattern of BOC.

accepted that CO_2 obtains an electron on the electrode and forms the intermediate $CO_2^{\bullet-}$.[19,20] Recently, Baruch et al. reported that the mechanism for the reduction of CO_2 to formate on Sn and In electrodes involves insertion of CO_2 at the electrode interface to form an electroactive surface-bound carbonate species, which is the first step in CO_2 conversion. They confirmed that carbonate is the intermediate for the reduction of CO_2 to formate on Sn and In electrodes using in situ attenuated total reflectance infrared spectroscopy.[21,22] These reports inspired us to design a catalyst containing a bonding carbonate (a possible intermediate for formate production), which may facilitate the CO_2 reduction reaction. Herein, we synthesized $Bi_2O_2CO_3$ (BOC) nanosheets as electrocatalysts for CO_2 reduction. Additionally, it is reported that nano-Bi metal catalysts can catalyze the reduction of CO_2 to formate with a high FE (92%) and good stability and can be obtained by the reduction of oxides of metal Bi.[23] Therefore, BOC decorated on a glassy carbon electrode (GCE) was reduced to metal Bi (RB), and a comparison of the performances of BOC and RB for CO_2 reduction was given.

2. RESULTS AND DISCUSSION

Figure 2a–c gives the morphologies of the prepared BOC. BOC shows a ruleless two-dimensional thin-sheet-like morphology and has a thickness ranging from 20 to 40 nm. The high-resolution transmission electron microscopy (HRTEM) image of BOC shows that the lattice spacing of 0.72 nm corresponds to the 110 crystallographic plane of BOC (see the inset of Figure 2c). The X-ray diffraction (XRD) pattern of the BOC sample is shown in Figure 2d, which is well indexed to the standard card of BOC (PDF No. 25-1464). No peaks of any other impurities were observed, indicating a high purity of the BOC sample.

Zhang et al. reported that nanosized Bi showed excellent performance for CO_2 reduction, and it was obtained from the electrochemical reduction of the metal oxide BiOCl.[23] In this article, the same method was used to reduce BOC to metal Bi (named RB) for making a comparison between the catalytic performances of BOC and RB.

Figure 3a shows the current–time curve during the electrochemical reduction of BOC at −1.5 V for 1 h. After the reduction process, the white BOC turned into black RB. The surface states of the BOC and RB catalysts were characterized by X-ray photoelectron spectroscopy (XPS). Figure 3b shows the high-resolution XPS spectra recorded for the Bi 4f region of BOC and RB. The valence state of Bi on the BOC catalyst surface is all Bi^{3+}. The Bi $4f_{7/2}$ spectra recorded for RB can fit to two components at 158.9 and 157.1 eV, which correspond to Bi^{3+} and Bi^0, respectively.[24] The peak area percentages of Bi^{3+} and Bi^0 are 92.3 and 7.7%, respectively. Through analysis of the XPS results, it can be realized that the main active substance of the surface of RB is BiO_x. Two possible reasons can explain the existence of Bi^{3+} on the surface of RB, which was obtained by the electrochemical reduction of BOC. First, because metal Bi is readily oxidized in air,[25] BiO_x may form quickly when RB modified on the GCE is exposed to air. Second, BOC is not fully reduced during the electrochemical process, which can be speculated by the reports that a metastable oxide layer presented on the surface of the Sn cathode even under reducing potentials.[22,26] Figure 3c shows

DOI: 10.1021/acsomega.7b00437
ACS Omega 2017, 2, 2561–2567

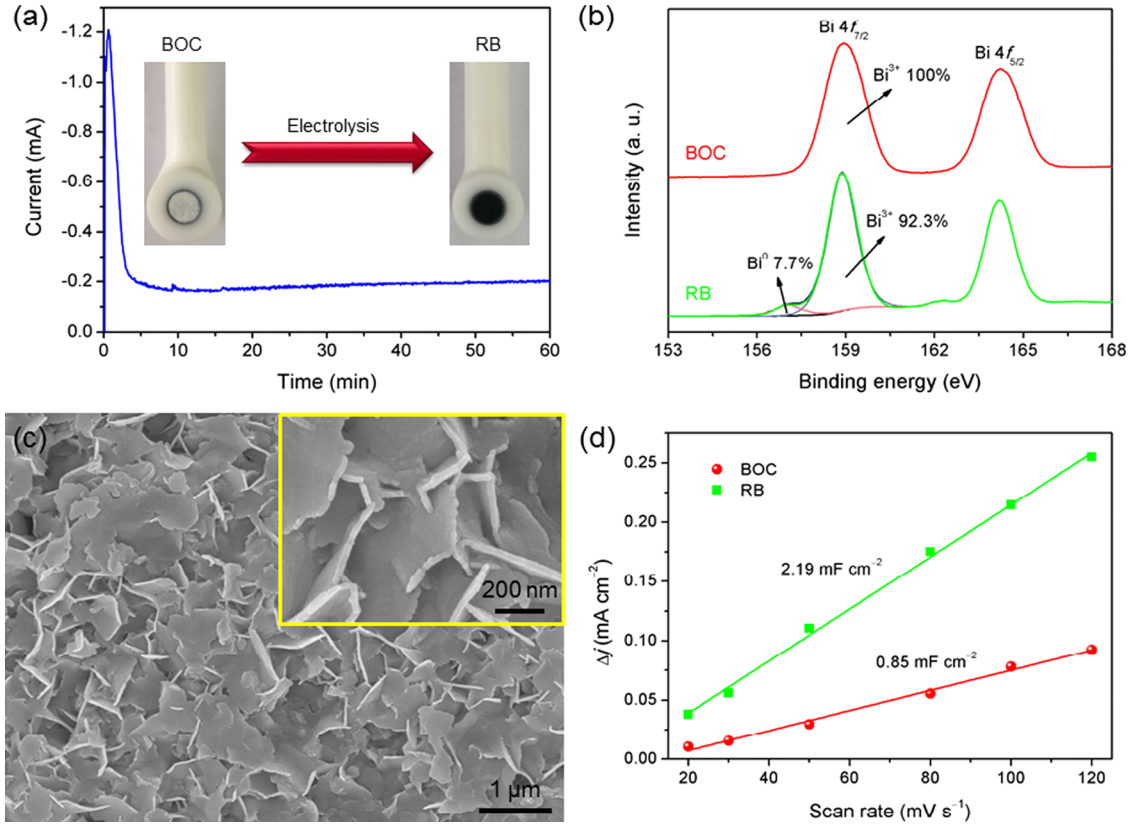

Figure 3. (a) Electrolysis current versus time during the electrochemical reduction of BOC to RB at −1.5 V; the insert images are photographs of the BOC- and RB-modified GCEs. (b) XPS spectra recorded for the Bi 4f region of BOC and RB. (c) SEM image of RB. (d) Charging current density differences of BOC and RB plotted against scan rates.

the morphology of RB. Compared with the BOC nanosheets in Figure 2a,b, the RB nanosheets have a similar thickness and adhered together, which is mainly due to the Nafion being mixed with RB on GCE. With the help of Nafion, the catalysts modified on the GCEs can remain stable during the electrolysis process. As shown in Figure 3d, the electrochemically active surface area (ECSA) of RB is around 2.5-fold that of BOC.

The electrolysis experiments were performed on BOC- and RB-modified GCEs, applying a constant potential in the range from −1.1 to −1.6 V. As shown by the FE for producing formate in Figure 4a, the FE of BOC reaches a maximum of 83% at −1.2 V. As has been mentioned, a low overpotential for the reaction of CO_2 reduction is desired for practical applications.[27−29] The overpotential (η) can be calculated by the equation

$$\eta = E^\circ - E(\text{vs Ag/AgCl}) - 0.20\ \text{V} \quad (1)$$

where E° is the standard electrode potential for the reduction of CO_2 to $HCOO^-$ (E° = −0.41 V vs that of the standard hydrogen electrode at pH 7.0).[30] In this work, the pH value of the electrolyte saturated with CO_2 was 6.98, which is very close to 7.0. The electrolysis potential of −1.2 V used in our experiments corresponds to the overpotential of 0.59 V. This result indicates that BOC is a very active catalyst for CO_2 reduction at a low overpotential. At more negative potentials, BOC has a lower FE than that of RB (Figure 4a). This is because BOC begins to be reduced at potentials lower than −1.2 V, which can be explained by the white BOC becoming black after electrolysis at potentials lower than −1.2 V. Because RB was formed by the reduction of BOC at −1.5 V, the FE for producing formate on BOC should be close to that for RB at this potential. It is surprising that the FE on BOC is much lower than that on RB at −1.5 V. Two reasons may explain this abnormal phenomenon. First, the total charge passed was 10 C during the electrolysis process. For the BOC-modified GCE, more than 0.77 C (calculated by Faraday's law) was consumed by the reaction of Bi^{3+} reduction ($Bi^{3+} + 3e^- = Bi$); this reaction may lead to a loss of ∼7.7% of the selectivity for formate production. Second, the RB-modified GCE has a different surface state compared to that of the BOC-modified GCE at −1.5 V. From the XPS analysis result (Figure 3b), we know that the main active substance on the surface of RB is BiO_x, and we believe that the amount of Bi^0 on the surface of the BOC-modified GCE during electrolysis at −1.5 V is higher than that on the surface of the RB-modified GCE because the BOC-modified GCE is immersed in the solution at all times, without being oxidized during the electrolysis process. In our previous work, we found that the metal Bi plate shows a low selectivity for formate production at −1.5 V.[31] Besides, when the BOC-modified GCE was reused for electrolysis at −1.5 V for the second time after it was exposed to air for ∼0.5 h, the FE was raised remarkably and reached up to 80%. Thus, we think that the different surface state is another reason for the low selectivity of BOC for formate production at −1.5 V.

Figure 4b illustrates the LSV curves of the BOC- and RB-modified GCEs in N_2- or CO_2-saturated 0.1 mol L^{-1} $KHCO_3$ solutions. For investigating the actual electrochemical behavior of BOC, the scanning potential is in the range of −0.6 to −1.2 V because BOC is reduced in situ to black RB when the potential is more negative than −1.2 V. As we know, the HER

DOI: 10.1021/acsomega.7b00437
ACS Omega 2017, 2, 2561−2567

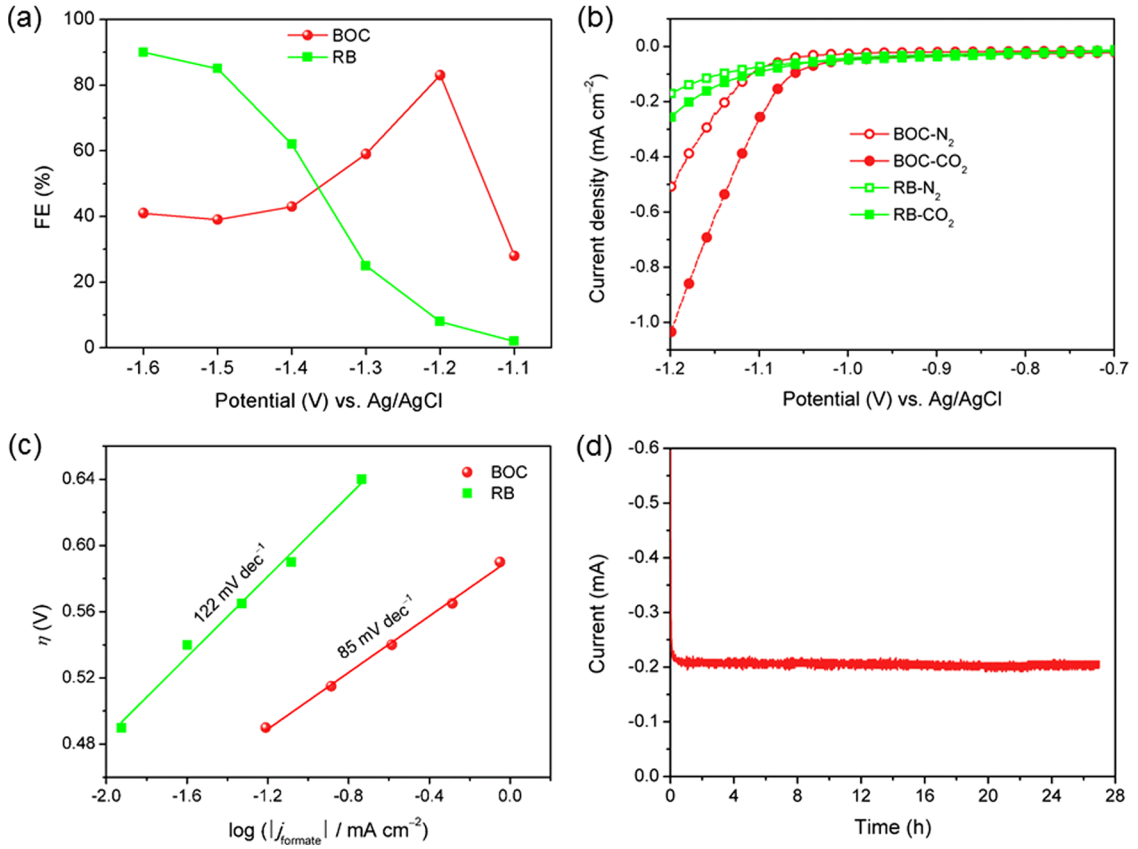

Figure 4. (a) Faradaic efficiency for producing formate versus electrolysis potential on the BOC- and RB-modified GCEs. (b) Linear sweep voltammetry (LSV) curves recorded on the BOC- and RB-modified GCEs in N_2-saturated (hollow) or CO_2-saturated (solid) 0.1 mol L^{-1} $KHCO_3$ solutions. (c) Tafel plots for producing formate on the BOC- and RB-modified GCEs. (d) Electrolysis current versus time during electrochemical reduction of CO_2 at −1.2 V on the BOC-modified GCE.

is a competitive reaction during the electrochemical reduction of CO_2 in an aqueous solution. As shown in Figure 4b, an obvious increase in the current densities can be observed at the cathodic end of the voltammograms under both N_2 and CO_2. Under N_2, this increase is mainly caused by the HER; under CO_2, the enhanced current must be caused by both the CO_2 reduction reaction and the HER. At a potential of −1.2 V, for BOC, the current density under CO_2 is significantly higher than that under N_2; for RB, the current density under CO_2 is only a little higher than that under N_2. This indicates that the CO_2 reduction reaction is more likely to occur on the BOC-modified GCE compared with the RB-modified GCE. On comparing the ECSA results of the two electrodes (Figure 3d), we found that the catalytic performances of the two electrodes are not due to their ECSAs. The Tafel plots for formate production on the BOC- and RB-modified GCEs were investigated, which are shown in Figure 4c. The resulting Tafel slope of BOC is only 85 mV $decade^{-1}$, which is much smaller than that of RB. The smaller Tafel slope of BOC is very advantageous for practical applications because it helps lower the rate-limiting activation energy barrier and hence remarkably increases the catalytic activity.[3] Continuous CO_2 reduction was performed at −1.2 V for 27 h to probe the durability of the BOC-modified GCE, and the result is shown in Figure 4d. The current does not obviously decay, and the FE for producing formate is always higher than 80% during the long test period. These observations indicate the favorable stability of the BOC-modified GCE. These results show that BOC is an ideal electrocatalyst for the reduction of CO_2 to formate with a high catalytic activity and stability.

As we known, a lower overpotential for the CO_2 reduction reaction is desired in practical application. As shown in Table 1, the overpotentials for the reduction of CO_2 to formate are higher than 1.0 V for most reported catalysts. Recently, some researchers reported some important results for the reduction of CO_2 to formate with low overpotentials. Among them, Min and Kanan reported that Pd nanoparticles dispersed on a

Table 1. Comparison of the Catalytic Performances of RB, BOC, and the Electrocatalysts Reported in the Literature for the Reduction of CO_2 to Formate

catalyst	overpotential (V)	FE (%)	current density (mA cm^{-2})	ref
metal (Sn, Pb, or In) plate	>1.10	>80	<5.0	12, 14, 19, 32
nano-Sn/graphene	1.12	93.6	10.2	11
Sn quantum sheets confined in graphene	1.14	89	21.1	3
porous Pb	1.04	88	<10.0	33
nano-Bi/Cu	0.89	91.3	3.1	31
RB	0.99	90	4.8	this work
BOC	0.59	83	1.0	this work
partially oxidized Co four-atom-thick layer	0.24	90	10.6	34
Pd/C	<0.20	99	3.0−5.5	30

DOI: 10.1021/acsomega.7b00437
ACS Omega 2017, 2, 2561−2567

carbon support can catalyze the reduction of CO_2 to formate with a high FE (even up to 99%) at an overpotential of less than 0.20 V, whereas Pd catalysts can deactivate due to the formation of CO, which poisons formate synthesis at a low overpotential.[30] Gao et al. reported that a partially oxidized four-atom-thick Co layer can catalyze the reduction of CO_2 to formate with a FE of 90% at an overpotential of 0.24 V; the excellent performance heavily depends on the ultrathin (0.84 nm) and partially oxidized Co layer structure.[34] In this work, the overpotentials of the RB and BOC catalysts are 0.99 and 0.59 V, respectively, which are lower than those of most traditional catalysts. Especially for the BOC catalyst, although its overpotential is not the lowest at present, easy preparation and high stability are its advantages. This contrast indicates that BOC is a promising catalyst for the reduction of CO_2 to formate.

Baruch et al. found that carbonate is the reaction intermediate for the reduction of CO_2 to formate.[21,22] If an electrocatalyst can form a complex with carbonate, it may decrease the overpotential for the reduction of CO_2 to formate by lowering the free energy of formation of the carbonate intermediate. According to this strategy, BOC was chosen as the electrocatalyst for the reduction of CO_2 to formate in this work because carbonate is already bonded in the structure of BOC, which likely takes part in the reaction as the intermediate. The proposed mechanism for the reduction of CO_2 to formate on the BOC catalyst is shown in Scheme 1. The first step is one

Scheme 1. Proposed Mechanism for the Reduction of CO_2 to Formate on the BOC Catalyst

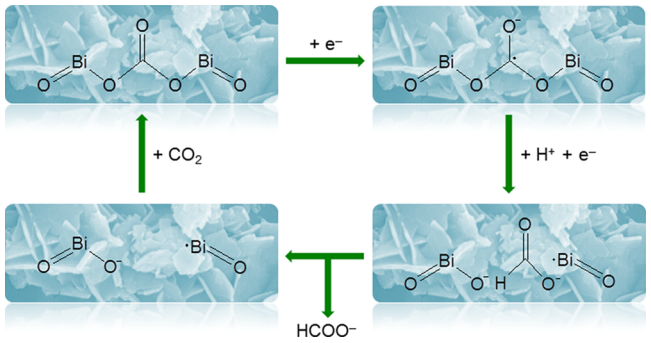

electron transfer to carbonate from BOC. Then, the initial carbonate in the structure of BOC converts to the formate anion by reacting with H^+ and adding another electron. Finally, the formate anion dissociates from the surface of BOC to the electrolyte. After that, BOC has a vacancy and can react with CO_2 and return to its initial state. It is interesting that the structure of this vacancy consists of $Bi^{\bullet}$ and O^-. $Bi^{\bullet}$ may adsorb an O atom of the CO_2 molecule, and O^- may adsorb the C atom of the CO_2 molecule. In this way, one CO_2 molecule can be adsorbed by two active sites at the same time, which may be beneficial for the reduction of CO_2 to formate. The advantage of the BOC electrocatalyst is that bonding carbonate can lower the energy barrier for the reduction of CO_2 to formate, which may decrease the overpotential of the reaction. This proposed mechanism is consistent with the above experimental results, which indicates that our strategy for designing the electrocatalyst is successful.

Currently, it is very challenging to characterize the right active sites of the catalysts.[35] The partially oxidized atomic Co layer (CoO_x/Co) is one of the most effective catalysts for the reduction of CO_2 to formate, but the reaction mechanism remains uncertain.[34] Inspired by the reaction mechanism in Scheme 1, the hybrid structure of the CoO_x/Co catalyst may also adsorb one CO_2 molecule with two active sites at the same time. It is reported that the surface structures of Sn, In, and Bi electrodes are also SnO_x/Sn, InO_x/In, and BiO_x/Bi, respectively,[12,21,36] whereas higher overpotentials are needed for the reduction of CO_2 to formate. This can be explained by the fact that the surface states of the outermost layers on Sn, In, and Bi are mainly the oxides and by the lack of synergy between metals and metal oxides. The surface oxide layer can only adsorb the C atom of the CO_2 molecule; this is not conducive for the conversion of the CO_2 molecule into the carbonate intermediate. Thus, the overpotentials for the reduction of CO_2 to formate on the Sn, In, and Bi electrodes are higher than those on BOC. We believe that the reaction mechanism in this work for the reduction of CO_2 to formate will pave the way toward the target-specific synthesis of highly active and stable catalysts. Further efforts are still needed to confirm the reaction pathway.

3. CONCLUSIONS

BOC nanosheets (20−40 nm thick) were synthesized for the electrochemical reduction of CO_2 to formate. RB was also prepared for comparing the catalytic performance toward CO_2 reduction to that of BOC. BOC showed a high activity and selectivity toward formate production at a low overpotential compared to those of RB. The maximum FE of BOC is 83% at −1.2 V, which is slightly lower than that of RB (90% obtained at −1.6 V), but the overpotential for the reduction of CO_2 to formate on BOC is lower than that on RB and most traditional catalysts. A long-time electrolysis experiment showed that the BOC electrocatalyst possesses a high stability for producing formate. We proposed a possible reaction mechanism on BOC. The carbonate of BOC, as the intermediate of the reduction of CO_2 to formate, is beneficial for lowering the overpotential of the reaction.

4. METHODS

4.1. Synthesis of the BOC Catalyst. All reagents were purchased from Sinopharm Chemical Reagent Co. Ltd. The procedure for preparing the BOC catalyst is as follows: 1 mmol $Bi(NO_3)_3{\cdot}5H_2O$ (dissolved in 20 mL of deionized water) and 50 mmol urea (dissolved in 20 mL of alcohol) were mixed together by magnetic stirring. After stirring for 30 min, the above mixture was heated to 90 °C for 4 h in a water bath and then cooled to room temperature. The resultant white BOC was collected by centrifugation, washed with deionized water and alcohol, and dried at 60 °C for 12 h.

4.2. Modified Electrode Preparation. BOC (20 mg) was first dispersed in 500 μL of alcohol under ultrasonication. Then, 50 μL of 5% Nafion solution was added to the suspension to form the sample solution during the ultrasound treatment process. Prior to each modification, an L-style GCE (5 mm in diameter) was polished with alumina powder, sonicated in alcohol and deionized water successively, and dried under nitrogen. Then, 10 μL of the as-prepared sample solution was cast onto the GCE and dried in air.

4.3. Electrochemical Experiments. The electrochemical experiments were performed in an undivided three-electrode glass cell with a Pt plate counter electrode (2 cm^2) and a Ag/AgCl reference electrode (saturated KCl). The working

DOI: 10.1021/acsomega.7b00437
ACS Omega 2017, 2, 2561−2567

electrode was the BOC-modified GCE. All potential values were in reference to those of the Ag/AgCl electrode. The electrolyte used was 20 mL of an aqueous solution of 0.1 mol L^{-1} $KHCO_3$.

LSV, with a scan rate of 50 mV s^{-1}, was carried out using a CHI 660E electrochemical workstation (Shanghai Chenhua Instruments Co., Ltd., China) in a N_2- or CO_2-saturated electrolyte (here, the electrolyte was bubbled with N_2 or CO_2 for 30 min prior to the measurement). The current density was determined on the area of the GCE. Controlled potential electrolysis was performed using a LAND CT2001C cell performance-testing instrument (Wuhan Electronics Co., Ltd., China). The electrolyte was saturated with CO_2 before the electrolysis experiment, and CO_2 gas was aerated continuously at a flow rate of 10 mL min^{-1} during the electrolysis process. The total charge passed was 10 C.

To acquire the ECSA of the working electrodes, their roughness factor (R_f) should be obtained first according to the equation ECSA = R_fS, where S is generally equal to the geometric area of the GCE (in this work, S = 0.196 cm^2). The R_f was determined by the relation $R_f = C_{dl}/60\ \mu F\ cm^{-2}$ on the basis of the double-layer capacitance (C_{dl}) of a smooth oxide surface (60 $\mu F\ cm^{-2}$). C_{dl} was estimated by plotting the charging current density differences (Δj) at −0.75 V against the scan rate, in which the slope was twice that of C_{dl}. $\Delta j = j_a - j_c$, where j_c and j_a are the cathodic and anodic current densities, respectively. Δj could be acquired by cyclic voltammetry measurements under the potential windows of −0.8 to −0.7 V (0.1 mol L^{-1} $KHCO_3$ aqueous solution).

4.4. Analysis and Calculations. The morphologies of BOC and RB were observed using a Hitachi S-4800 SEM. The TEM observation was carried out using a JEOL JEM-2100F TEM instrument. The XRD pattern of BOC was obtained with a Bruker D8 Advance powder X-ray diffractometer using Cu Kα radiation (wavelength λ = 0.15406 nm). The valence state of Bi on the surfaces of the electrocatalysts was quantified by an ESCALAB 250Xi XPS instrument. Ion chromatography (IC) was employed to quantify the concentration of the formate product in the aqueous solutions. The IC data was obtained using a Dionex ICS-5000$^+$ ion chromatography instrument.

The FE for producing formate can be determined by the equation

$$FE = 2nF/Q \quad (2)$$

where n is the number of moles of the formate product, which can be calculated according to the IC data, F is Faraday's constant, with a value of 96 485 C mol^{-1}, and Q is the total charge passed during electrolysis (here, Q = 10 C).

AUTHOR INFORMATION

Corresponding Authors

*E-mail: zhangrui@ycit.cn (R.Z.).
*E-mail: wangw@ycit.edu.cn (W.W.).

ORCID

Rui Zhang: 0000-0003-3404-6800

Notes

The authors declare no competing financial interest.

ACKNOWLEDGMENTS

This work was supported by the National Natural Science Foundation of China (Nos. 21603184, 21675139, and 21575123), the Industry-University-Research Cooperative Innovation Foundation of Jiangsu Province (No. BY2015057-17), and the joint research fund between the Collaborative Innovation Center for Ecological Building Materials and Environmental Protection Equipments and Key Laboratory for Advanced Technology in Environmental Protection of Jiangsu Province.

REFERENCES

(1) Aresta, M.; Dibenedetto, A.; Angelini, A. Catalysis for the valorization of exhaust carbon: from CO_2 to chemicals, materials, and fuels. Technological use of CO_2. *Chem. Rev.* **2014**, *114*, 1709−1742.

(2) Asadi, M.; Kim, K.; Liu, C.; Addepalli, A. V.; Abbasi, P.; Yasaei, P.; Phillips, P.; Behranginia, A.; Cerrato, J. M.; Haasch, R.; Zapol, P.; Kumar, B.; Klie, R. F.; Abiade, J.; Curtiss, L. A.; Salehi-Khojin, A. Nanostructured transition metal dichalcogenide electrocatalysts for CO_2 reduction in ionic liquid. *Science* **2016**, *353*, 467−470.

(3) Lei, F.; Liu, W.; Sun, Y.; Xu, J.; Liu, K.; Liang, L.; Yao, T.; Pan, B.; Wei, S.; Xie, Y. Metallic tin quantum sheets confined in graphene toward high-efficiency carbon dioxide electroreduction. *Nat. Commun.* **2016**, *7*, 12697.

(4) Wang, W. H.; Himeda, Y.; Muckerman, J. T.; Manbeck, G. F.; Fujita, E. CO_2 hydrogenation to formate and methanol as an alternative to photo- and electrochemical CO_2 reduction. *Chem. Rev.* **2015**, *115*, 12936−12973.

(5) Yin, Z.; Gao, D. F.; Yao, S. Y.; Zhao, B.; Cai, F.; Lin, L. L.; Tang, P.; Zhai, P.; Wang, G. X.; Ma, D.; Bao, X. H. Highly selective palladium-copper bimetallic electrocatalysts for the electrochemical reduction of CO_2 to CO. *Nano Energy* **2016**, *27*, 35−43.

(6) Li, Q.; Zhu, W. L.; Fu, J. J.; Zhang, H. Y.; Wu, G.; Sun, S. H. Controlled assembly of Cu nanoparticles on pyridinic-N rich graphene for electrochemical reduction of CO_2 to ethylene. *Nano Energy* **2016**, *24*, 1−9.

(7) Zhang, Y. J.; Sethuraman, V.; Michalsky, R.; Peterson, A. A. Competition between CO_2 reduction and H_2 evolution on transition-metal electrocatalysts. *ACS Catal.* **2014**, *4*, 3742−3748.

(8) Lee, C. H.; Kanan, M. W. Controlling H^+ vs CO_2 reduction selectivity on Pb electrodes. *ACS Catal.* **2015**, *5*, 465−469.

(9) Surya Prakash, G. K.; Viva, F. A.; Olah, G. A. Electrochemical reduction of CO_2 over Sn-Nafion coated electrode for a fuel-cell-like device. *J. Power Sources* **2013**, *223*, 68−73.

(10) Lv, W. X.; Zhou, J.; Kong, F. Y.; Fang, H. L.; Wang, W. Porous tin-based film deposited on copper foil for electrochemical reduction of carbon dioxide to formate. *Int. J. Hydrogen Energy* **2016**, *41*, 1585−1591.

(11) Zhang, S.; Kang, P.; Meyer, T. J. Nanostructured tin catalysts for selective electrochemical reduction of carbon dioxide to formate. *J. Am. Chem. Soc.* **2014**, *136*, 1734−1737.

(12) Zhang, R.; Lv, W. X.; Lei, L. X. Role of the oxide layer on Sn electrode in electrochemical reduction of CO_2 to formate. *Appl. Surf. Sci.* **2015**, *356*, 24−29.

(13) Wu, J. J.; Risalvato, F. G.; Ma, S.; Zhou, X. D. Electrochemical reduction of carbon dioxide III. The role of oxide layer thickness on the performance of Sn electrode in a full electrochemical cell. *J. Mater. Chem. A* **2014**, *2*, 1647−1651.

(14) Lv, W. X.; Zhang, R.; Gao, P. R.; Lei, L. X. Studies on the faradaic efficiency for electrochemical reduction of carbon dioxide to formate on tin electrode. *J. Power Sources* **2014**, *253*, 276−281.

(15) Wu, J. J.; Sun, S. G.; Zhou, X. D. Origin of the performance degradation and implementation of stable tin electrodes for the conversion of CO_2 to fuels. *Nano Energy* **2016**, *27*, 225−229.

(16) Wu, J. J.; Sharma, P. P.; Harris, B. H.; Zhou, X. D. Electrochemical reduction of carbon dioxide: IV dependence of the Faradaic efficiency and current density on the microstructure and thickness of tin electrode. *J. Power Sources* **2014**, *258*, 189−194.

(17) Zhang, R.; Lv, W. X.; Li, G. H.; Mezaal, M. A.; Li, X. J.; Lei, L. X. Retarding of electrochemical oxidation of formate on the platinum anode by a coat of Nafion membrane. *J. Power Sources* **2014**, *272*, 303−310.

DOI: 10.1021/acsomega.7b00437
ACS Omega 2017, 2, 2561−2567

(18) Rosen, B. A.; Salehi-Khojin, A.; Thorson, M. R.; Zhu, W.; Whipple, D. T.; Kenis, P. J. A.; Masel, R. I. Ionic liquid−mediated selective conversion of CO_2 to CO at low overpotentials. *Science* **2011**, *334*, 643−644.
(19) Lu, X.; Leung, D. Y. C.; Wang, H.; Leung, M. K. H.; Xuan, J. Electrochemical reduction of carbon dioxide to formic acid. *ChemElectroChem* **2014**, *1*, 836−849.
(20) Zhu, D. D.; Liu, J. L.; Qiao, S. Z. Recent advances in inorganic heterogeneous electrocatalysts for reduction of carbon dioxide. *Adv. Mater.* **2016**, *28*, 3423−3452.
(21) Detweiler, Z. M.; White, J. L.; Bernasek, S. L.; Bocarsly, A. B. Anodized indium metal electrodes for enhanced carbon dioxide reduction in aqueous electrolyte. *Langmuir* **2014**, *30*, 7593−7600.
(22) Baruch, M. F.; Pander, J. E.; White, J. L.; Bocarsly, A. B. Mechanistic insights into the reduction of CO_2 on tin electrodes using in situ ATR-IR spectroscopy. *ACS Catal.* **2015**, *5*, 3148−3156.
(23) Zhang, H.; Ma, Y.; Quan, F.; Huang, J. J.; Jia, F. L.; Zhang, L. Z. Selective electro-reduction of CO_2 to formate on nanostructured Bi from reduction of BiOCl nanosheets. *Electrochem. Commun.* **2014**, *46*, 63−66.
(24) Medina-Ramos, J.; DiMeglio, J. L.; Rosenthal, J. Efficient reduction of CO_2 to CO with high current density using in situ or ex situ prepared Bi-based materials. *J. Am. Chem. Soc.* **2014**, *136*, 8361−8367.
(25) Zhang, Z.; Chi, M.; Veith, G. M.; Zhang, P.; Lutterman, D. A.; Rosenthal, J.; Overbury, S. H.; Dai, S.; Zhu, H. Rational design of Bi nanoparticles for efficient electrochemical CO_2 reduction: the elucidation of size and surface condition effects. *ACS Catal.* **2016**, *6*, 6255−6264.
(26) Chen, Y. H.; Kanan, M. W. Tin oxide dependence of the CO_2 reduction efficiency on tin electrodes and enhanced activity for tin/tin oxide thin-film catalysts. *J. Am. Chem. Soc.* **2012**, *134*, 1986−1989.
(27) Min, S. X.; Yang, X. L.; Lu, A. Y.; Tseng, C. C.; Hedhili, M. N.; Li, L. J.; Huang, K. W. Low overpotential and high current CO_2 reduction with surface reconstructed Cu foam electrodes. *Nano Energy* **2016**, *27*, 121−129.
(28) Torelli, D. A.; Francis, S. A.; Crompton, J. C.; Javier, A.; Thompson, J. R.; Brunschwig, B. S.; Soriaga, M. P.; Lewis, N. S. Nickel-Gallium-catalyzed electrochemical reduction of CO_2 to highly reduced products at low overpotentials. *ACS Catal.* **2016**, *6*, 2100−2104.
(29) Taheri, A.; Thompson, E. J.; Fettinger, J. C.; Berben, L. A. An iron electrocatalyst for selective reduction of CO_2 to formate in water: including thermochemical insights. *ACS Catal.* **2015**, *5*, 7140−7151.
(30) Min, X.; Kanan, M. W. Pd-catalyzed electrohydrogenation of carbon dioxide to formate: high mass activity at low overpotential and identification of the deactivation pathway. *J. Am. Chem. Soc.* **2015**, *137*, 4701−4708.
(31) Lv, W. X.; Zhou, J.; Bei, J. J.; Zhang, R.; Wang, L.; Xu, Q.; Wang, W. Electrodeposition of nano-sized bismuth on copper foil as electrocatalyst for reduction of CO_2 to formate. *Appl. Surf. Sci.* **2017**, *393*, 191−196.
(32) Hori, Y. Electrochemical CO_2 Reduction on Metal Electrodes. In *Modern Aspects of Electrochemistry*; Vayenas, C. G., White, R. E., Gamboa-Aldeco, M. E., Eds.; Springer: New York, 2008; pp 89−189.
(33) Wang, J.; Wang, H.; Han, Z. Z.; Han, J. Y. Electrodeposited porous Pb electrode with improved electrocatalytic performance for the electroreduction of CO_2 to formic acid. *Front. Chem. Sci. Eng.* **2014**, *9*, 57−63.
(34) Gao, S.; Lin, Y.; Jiao, X. C.; Sun, Y. F.; Luo, Q. Q.; Zhang, W. H.; Li, D. Q.; Yang, J. L.; Xie, Y. Partially oxidized atomic cobalt layers for carbon dioxide electroreduction to liquid fuel. *Nature* **2016**, *529*, 68−71.
(35) Zhu, Y.; Zhang, B.; Liu, X.; Wang, D. W.; Su, D. S. Unravelling the structure of electrocatalytically active Fe−N complexes in carbon for the oxygen reduction reaction. *Angew. Chem., Int. Ed.* **2014**, *53*, 10673−10677.
(36) Bei, J.; Zhang, R.; Chen, Z.; Lv, W.; Wang, W. Efficient reduction of CO_2 to formate Using in situ prepared nano-sized Bi electrocatalyst. *Int. J. Electrochem. Sci.* **2017**, *12*, 2365−2375.

DOI: 10.1021/acsomega.7b00437
ACS Omega 2017, 2, 2561−2567